Published online 16 April 2007

Nucleic Acids Research, 2007, Vol. 35, No. 9 ***2965–2974***
doi:10.1093/nar/gkm184

Thermodynamics and kinetics for base-pair opening in the P1 duplex of the *Tetrahymena* group I ribozyme

Joon-Hwa Lee[1,2] and Arthur Pardi[1,*]

[1]Department of Chemistry and Biochemistry, University of Colorado at Boulder, Boulder, CO 80309-0215, USA and [2]Department of Chemistry and Research Institute of Natural Science, Gyeongsang National University, Jinju, Gyeongnam 660-701, Republic of Korea

Received January 22, 2007; Revised and Accepted March 14, 2007

ABSTRACT

The thermodynamics and kinetics for base-pair opening of the P1 duplex of the *Tetrahymena* group I ribozyme were studied by NMR hydrogen exchange experiments. The apparent equilibrium constants for base pair opening were measured for most of the imino protons in the P1 duplex using the base catalysts NH_3, HPO_4^{2-} or TRIS. These equilibrium constants were also measured for several modified P1 duplexes, and the C-2·G23 base pair was the most stable base pair in all the duplexes. The conserved U-1·G22 base pair is required for activity of the ribozyme and the data here show that this wobble base pair destabilizes neighboring base pairs on only one side of the wobble. A 2′-OMe modification on the U-3 residue stabilized its own base pair but had little effect on the neighboring base pairs. Three base pairs, U-1·G22, C-2·G23 and A2·U21 showed unusual equilibrium constants for opening and possible implications of the opening thermodynamics of these base pairs on the undocking rates of the P1 helix with catalytic core are discussed.

INTRODUCTION

The *Tetrahymena* group I intron has been a powerful model system for studying conformational changes in RNA and for understanding the catalytic potential of RNA (1–3). The *Tetrahymena* L-21 ScaI ribozyme is derived from the self-splicing group I intron and catalyzes a transesterification reaction as part of the self-splicing reaction (1,4). The internal guide sequence (IGS; 3′-GGAGGG—ribozyme) in the ribozyme forms the P1 duplex with a substrate, for example 5′-CCCUCUpA. The ribozyme also binds exogenous guanosine which reacts with the substrate to yield GpA and CCCUCU (1). Cleavage rates have been measured on a large number of modified substrates or ribozymes, from which it was proposed that the catalytic reaction is mediated by three divalent metal ions at the active site of the ribozyme (2–12). Additional kinetics studies showed that the P1 duplex docks into the catalytic core by a two-step reaction: the first step involves formation of the P1 duplex, where the substrate binds to the IGS of the ribozyme and subsequent formation of a closed complex, where the P1 duplex docks into the catalytic core of ribozyme (1,9,13). Various modifications of the substrate or the IGS have been shown to affect the cleavage kinetics and/or the thermodynamics and kinetics for docking of the P1 duplex into the catalytic core (1,3,7). For example, a DNA substrate binds the ribozyme with 10 000-fold lower affinity than an RNA substrate and is cleaved 10 000 times slower than an RNA substrate (6,14,15). Biochemical studies showed that the 2′-OH groups at positions 22, 25 and –3 on the P1 duplex are important for stabilizing tertiary interactions with the catalytic core of ribozyme (1,12). A dU modification at position −1 of the substrate also reduced the cleavage rate (3) but had no effect on the docking/undocking rates (7). Replacing the conserved U-1·G22 wobble pair with a Watson–Crick C-1·G22 pair leads to a large (~80-fold) increase in the undocking rate and 2′-OMe modifications at positions −1 or –3 also increased the undocking rates, 20- or 140-fold, respectively (7).

X-ray crystal structures of the group I intron from several species have been reported (16–18) and these structures have been very useful in the interpretation of previous biochemical and biophysical studies (19,20). However, even with these X-ray structures it is not clear whether the changes in cleavage activity observed for a specific modification are due to changes in conformation, changes in dynamics or flexibility of the RNA or a redistribution of the populations of various conformational states. NMR hydrogen exchange

*To whom correspondence should be addressed. Tel: +1-303-492-6263; Fax: +1-303-492-5894; Email: Arthur.Pardi@colorado.edu

experiments are used here to probe the conformational dynamics of the isolated P1 duplex for the *Tetrahymena* ribozyme with the goal of better understanding specific properties of the P1 duplex that are required for catalytic activity.

NMR hydrogen exchange experiments provide information on the thermodynamics and kinetics for base-pair opening and therefore represent a probe of the dynamic motions of the base pairs. These experiments have been used to probe base-pair opening in various DNAs (21–25), RNAs (25,26) and DNA–protein complexes (27,28). Analysis of the hydrogen exchange of imino protons generally employs a two-state (open/closed) model for the base pair, where hydrogen exchange only occurs from the open state (29–31). The opening/closing rate constants and/or equilibrium constant for base-pair opening can often be determined by measuring the exchange as a function of the concentration of external catalyst. Hydrogen exchange data can also be used to probe how intramolecular or intermolecular interactions stabilize nucleic acid duplexes. For example, NMR imino proton exchange studies of a DNA duplex bound to the enzyme DNA glycosylase showed that the enzyme substantially increases the equilibrium constant for opening an A·T base pair without changing the rate constant for base-pair opening (28).

The imino proton exchange rates were measured here for a model P1 RNA duplex formed by an 11-nt IGS, 5′-GGUUUGGAGGG-3′ and a 13-nt wild-type (wt) substrate, 5′-GGCCCUCUAAACC-3′ (Figure 1A). The equilibrium constants for opening of the two most stable base pairs in the P1 duplex, C-2·G23 and C-4·G25, were determined from measurements of imino proton exchange rates as a function of the concentration of the base catalyst ammonia at 35°C. The less effective base catalysts, HPO_4^{2-} or TRIS base, were also used to estimate the equilibrium constants for opening of base pairs for the more rapidly exchanging imino protons in the P1 duplex. These data show that the U-1·G22 wobble in the P1 duplex has a large effect on the equilibrium constants for opening of this base pair, and also asymmetrically affects the equilibrium constants for opening of neighboring base pairs. To further understand the correlation between the base-pair opening and changes in biochemical properties and function of the P1 duplex in the *Tetrahymena* ribozyme, the equilibrium constants for base-pair opening were measured in a number of previously biochemically characterized modified P1 duplexes (see Figure 1A). Comparison of the wt and modified P1 duplexes indicates that some differences in base-pair opening properties are correlated with changes in undocking rates of the P1 duplex into the catalytic core of the ribozyme.

MATERIALS AND METHODS

Sample preparation

The sequence of the wt and three modified P1 duplexes employed here are given in Figure 1A. The substrate strands for the wt and the (-5U)-P1 duplexes were

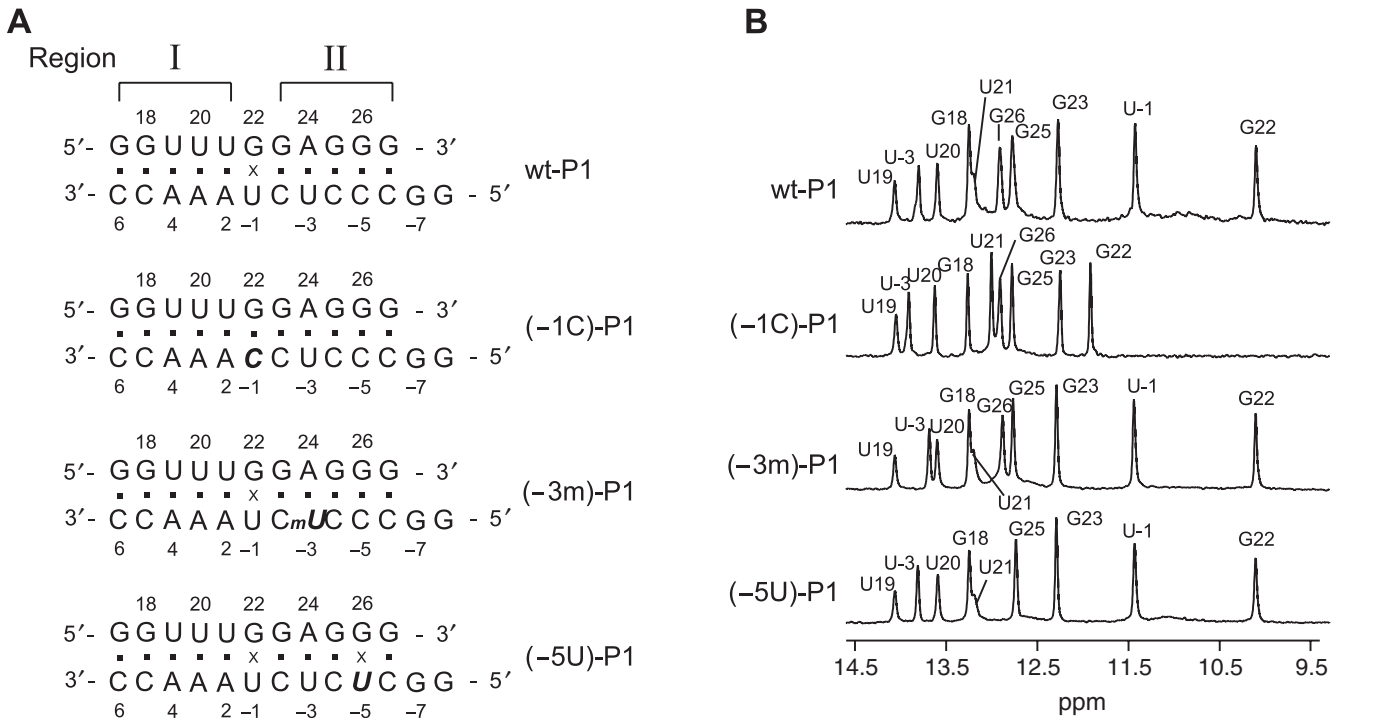

Figure 1. (**A**) The sequences of the wt P1, (-1C)-P1, (-3m)-P1 and (-5U)-P1 duplexes. The numbering of the P1 duplexes follows that of the *Tetrahymena* group I intron. The modifications are indicated by italic and bold characters. The top strand is the IGS in the ribozyme and bottom strand is the substrate. The P1 helix can be divided into an A·U-rich region (denoted region I) and a G·C-rich region (denoted region II) around the central G·U base pair (**B**) 1D imino proton spectra of the wt P1, (-1C)-P1, (-3m)-P1 and (-5U)-P1 duplexes dissolved in NMR buffer at 35°C. The resonance assignments for the imino protons were made from analysis of 2D NOESY spectra.

prepared by *in vitro* transcription as previously described (32). The other oligomers, the IGS-11mer and the substrates for the (-1C)- and (-3m)-P1 duplexes were purchased from Dharmacon, Inc. (Lafayette, CO) or the W.M. Keck facility at Yale University (New Haven, CT). The oligomers were desalted using NAP 5 columns (Amersham Biosciences, NJ), and ~0.5–0.9 mM RNA duplex samples were formed by combining molar equivalents of IGS and the appropriate substrate in 90% H_2O–10% D_2O NMR buffer (10 mM sodium phosphate, 100 mM NaCl, 10 mM $MgCl_2$, 0.1 mM EDTA, pH 6.6). The duplexes were then dialyzed to achieve specific buffer conditions using Microsep 1K concentrators (PALL Life Sciences, MI). The pH of each sample was measured directly by using a micro-combination electrode (Fisher Scientific), except for samples containing TRIS buffer. To account for the change in the pK_a of TRIS with temperature, the pH of the solution was directly measured at room temperature (23.4°C) and then the pH of the NMR sample at 35°C was calculated using the relation between pK_a of TRIS and temperature, $\Delta pK_a = -0.033 \times \Delta T$ (33).

Analysis of imino proton exchange

The formalism of catalyzed proton exchange has been previously described in detail (30,31), and is briefly presented here. The rate constant for imino proton exchange, k_{tr}, induced by a base (proton acceptor) in an isolated nucleoside is:

$$k_{tr} = k_i[B] = \frac{k_{coll}[B]}{1 + 10^{\Delta pK_a}} \quad \mathbf{1}$$

where k_i is the rate constant for imino proton transfer, k_{coll} is the collision rate constant, [B] is the base catalyst concentration and ΔpK_a is the pK_a difference between the imino proton and the base.

Imino proton exchange from a base pair was analyzed by the two-step process, base-pair opening followed by proton transfer to a base such as NH_3 or TRIS. The base catalyst contribution to the rate constant for imino proton exchange, $k_{ex,B}$, is given by

$$k_{ex,B} = \frac{k_{op}k_{tr}}{k_{cl} + k_{tr}} = \frac{\alpha K_{op} k_i[B]}{1 + \alpha K_{op} k_i[B]/k_{op}} \quad \mathbf{2}$$

where k_{op} and k_{cl} are the rate constants for opening and closing of the base pair, respectively, and k_{tr} is the rate constant for proton exchange by base catalyst in the open state [see Equation (1)], α is called the accessibility factor (30), and K_{op} ($= k_{op}/k_{cl}$) is the equilibrium constant for base-pair opening [note that this is referred to as K_d by Guéron and coworkers (30,31)].

In the absence of added catalysts, exchange is due to a concerted transfer involving water molecules bridging the imino proton and the nitrogen of the complementary base, which acts as an intrinsic (or internal) catalyst (30). The rate constant for imino proton exchange in the absence of added catalyst, k_{ACC}, is

$$k_{ex} = k_{ACC} = \frac{k_{op}k^{ACC}_{tr,open}}{k_{cl} + k^{ACC}_{tr,open}} \quad \mathbf{3}$$

where $k^{ACC}_{tr,open}$ is the rate constant for imino proton transfer by intrinsic base catalyst, and this rate constant is in the range of $10^6\,s^{-1}$ (30). When k_{cl} is larger than $k^{ACC}_{tr,open}$, Equation (3) becomes:

$$k_{ACC} = K_{op}k^{ACC}_{tr,open} \quad \mathbf{4}$$

NMR spectroscopy

All NMR experiments were performed on Varian Inova 500 MHz spectrometer using a HCN triple-resonance probe equipped with *z*-axis pulsed-field gradients. 1D data were processed with the program FELIX (Accelrys), 2D data were processed with the program NMRPIPE (34) and analyzed by the program Sparky (35). The imino protons in the various P1 duplexes are assigned using 120 and 200 ms Watergate-NOESY or jump-return-echo-NOESY spectra acquired at 15 and 35°C. The apparent longitudinal relaxation rate constants ($R_{1a} = 1/T_{1a}$) of the imino protons were determined by semi-selective inversion recovery 1D NMR experiments, where a semi-selective 180° inversion pulse was applied to imino proton region (9–15.5 p.p.m.) before the jump-return-echo water suppression pulse (29). The apparent relaxation rate constant of water (R_{1w}) was determined by a selective inversion recovery experiment, using a DANTE sequence for selective water inversion and application of a 1-ms gradient (4 G/cm) after the DANTE pulse and a weak gradient (0.02 G/cm) during the relaxation delay to avoid radiation damping of water signals (29). The probe was detuned for this experiment to help reduce the large water signal. The R_{1a} and R_{1w} were determined by curve fitting of the inversion recovery data to the appropriate single exponential function. The R_{1w} of water containing 90% H_2O–10% D_2O 10 mM sodium phosphate (pH 6.6) in NMR buffer was $0.274\,s^{-1}$ at 35°C at 500 MHz. The hydrogen exchange rates of the imino protons were measured by a water magnetization transfer experiment at 35°C, where a selective 180° pulse for water was applied, followed by a variable delay, and then a 3–9–19 acquisition pulse was used to suppress the water signal (29,36). During the delay times between selective water inversion and acquisition pulses, a weak gradient (0.02 G/cm) was applied to prevent the radiation damping of the water signal. The intensities of each imino proton were measured with 20 different delay times ranging from 5 to 100 ms (see Figure 2). The exchange rates were determined by fitting the relative peak intensities, $I(t)/I_0$, of the imino protons to:

$$\frac{I(t)}{I_0} = 1 - 2\frac{k_{ex}}{(R_{1w} - R_{1a})}\left(e^{-R_{1a}t} - e^{-R_{1w}t}\right) \quad \mathbf{5}$$

where R_{1a} and R_{1w} were previously measured by inversion recovery experiments, k_{ex} is the rate constant for exchange of the imino proton, and I_0 and $I(t)$ are the peak intensities of the imino proton at times zero and t, respectively (29).

Determination of the apparent equilibrium constant for base-pair opening

The apparent relaxation rate constant for an imino proton is the summation of the R_1 rate constant, which is the

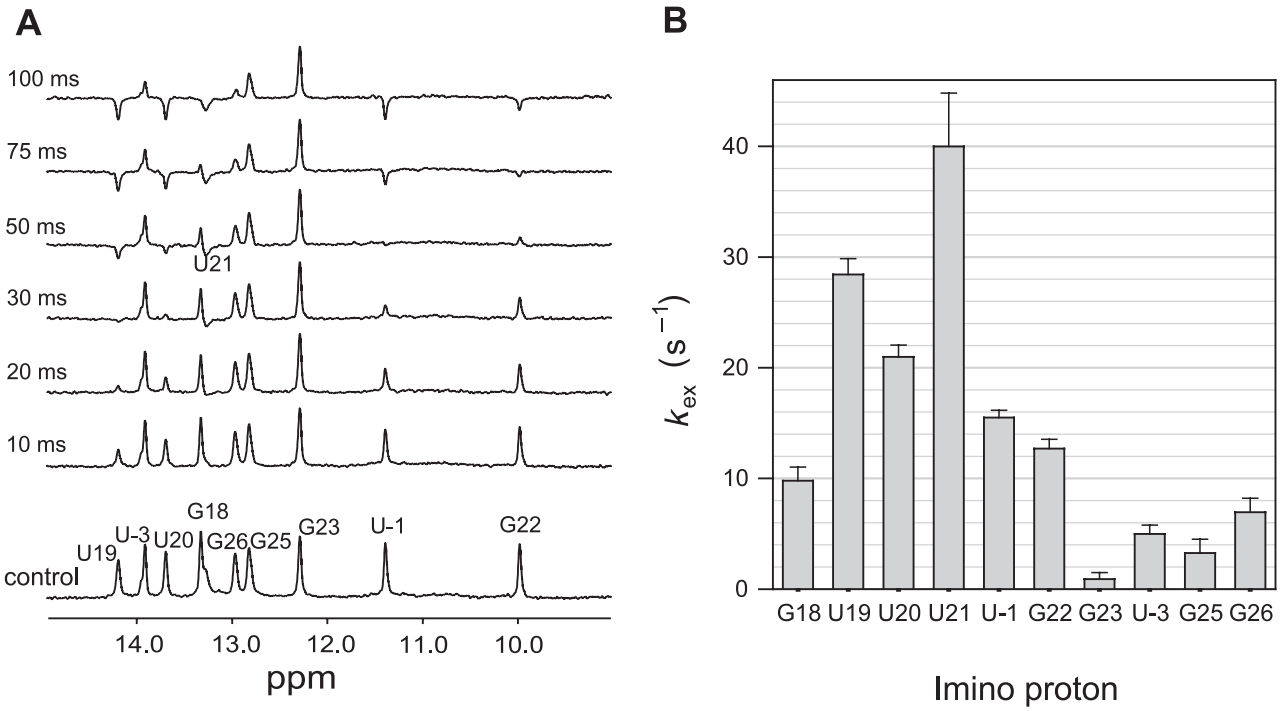

Figure 2. (**A**) 1D spectra of the water magnetization transfer experiments showing the imino protons of the wt P1 duplex in NMR buffer at 35°C. The control spectrum with no selective water inversion is shown at the bottom with resonance assignments. The delay times between the selective water inversion and acquisition pulses are indicated on the left side of the spectra. The inter-acquisition delay was set to 15 s which allows for complete relaxation of the water magnetization. (**B**) The rate constants for exchange of the imino protons for the P1 duplex at 35°C determined by fitting to Equation (5), and the error bars represents fitting errors.

inverse of T_1 spin-lattice relaxation time of this proton, and the rate constant for imino proton exchange. It is assumed that the R_1 values of the imino protons are not affected by the addition of the base catalyst such as ammonia, TRIS or HPO_4^{2-}. Thus, the apparent relaxation rate constant, R_{1a}, for an imino proton is given by:

$$R_{1a} = R_1 + k_{ex} = R_1 + k_{ACC} + k_{ex,B} \quad \mathbf{6}$$

where R_1 is the relaxation rate constant of the imino proton and k_{ACC} and $k_{ex,B}$ are the contribution to imino proton exchange of the intrinsic base and the added base catalyst, respectively. Substituting Equation (2) into Equation (6) yields the following:

$$R_{1a} = R_1 + k_{ACC} + \frac{\alpha K_{op} k_i[B]}{1 + \alpha K_{op} k_i[B]/k_{op}} = R_1 + k_{ACC} + \frac{\alpha k_{op} k_i[B]}{k_{cl} + \alpha k_i[B]} \quad \mathbf{7}$$

and curve fitting R_{1a} of the imino protons as a function of the base catalyst concentration with Equation (7) (using Sigmaplot) gives the apparent equilibrium constant for base-pair opening (αK_{op}) and rate constant for opening (k_{op}); where the k_i for each base catalyst was calculated using Equation (1). In these fits, all the R_{1a} values were weighted by their inverse variances. Under certain conditions where k_{cl} ($=k_{op}/K_{op}$) is much larger than $\alpha k_i[B]$, Equation (7) simplifies to:

$$R_{1a} = R_1 + k_{ACC} + \alpha K_{op} k_i[B] \quad \mathbf{8}$$

RESULTS

Resonance assignment of imino protons in the P1 duplexes

The 1D imino proton spectra of the wt and modified P1 duplexes at 35°C are shown in Figure 1B, and assignments were made by the analysis of NOESY spectra at 35°C. The three other modified P1 duplexes were assigned by comparison of their NOESY spectra with the wt P1 duplex. All imino proton resonances except G18 and U21 imino protons are well resolved in the 1D spectra (Figure 1B). 1D imino proton spectra of the wt P1 duplex were collected as a function of temperature and the resonances for all the non-terminal base pairs are still observed up to 50°C (data not shown).

Relaxation and hydrogen exchange experiments for the imino protons in the wt P1 duplex

The apparent longitudinal relaxation rate constants (R_{1a}) of the imino protons of the P1 duplex were determined by semi-selective inversion recovery experiments on the imino proton resonances. At 15°C, the R_{1a} data for the imino proton resonances did not fit well to a single exponential and all showed unusual double exponential relaxation (see Supplementary Data Figure 6S, left column). This behavior may result from partial aggregation of the P1 duplex at low temperature. However, inversion recovery relaxation data for all the imino protons fit well to single exponentials at 35°C, (see Supplementary Data Figure 6S, right column), thus the exchange

properties of the imino protons for all the P1 duplexes were determined from experiments at 35°C.

Hydrogen exchange rates were determined from water magnetization transfer experiments on the imino protons for the wt P1 duplex at 35°C as described in Materials and Methods section. Some imino protons show large differences in peak intensities as a function of delay after water inversion (Figure 2). For example, rapidly exchanging imino protons such as U19 and U20 show negative peaks at short delay times (50 ms in Figure 2A), whereas the G23 resonance, which is the slowest exchanging imino proton, remains basically unchanged up to 100 ms. Figure 2B shows the k_{ex} of the imino protons of the P1 duplex determined by the curve fitting to Equation (5) (see Materials and Methods). The G and U imino protons in the A·U-rich region (region I in Figure 1A) have k_{ex} from 9 to 40 s^{-1}, whereas, except for the terminal base pairs, the imino protons in the G·C-rich region (region II) all have $k_{ex} < 6\,s^{-1}$. The U21 imino proton next to the central G·U pair has the largest rate constant for exchange of any non-terminal base pair (k_{ex} of $40.0 \pm 4.8\,s^{-1}$), and the G22 and U-1 imino protons of the central G·U wobble pair have k_{ex} values of 12.7 ± 0.8 and $15.5 \pm 0.7\,s^{-1}$, respectively. As seen in Figure 2B, the central G·U wobble pair has a larger effect on k_{ex} for base pairs in region I than region II. The most striking result is that the G23 imino proton is the slowest exchanging proton in the P1 duplex, even though the C-2·G23 base pair is flanked on one side by a relatively rapidly exchanging U-1·G22 base pair and on the other by only a moderately exchanging U-3·A24 base pair.

Base-pair opening stability and kinetics for the P1 duplexes with NH_3 or HPO_4^{2-} base catalysts

The apparent equilibrium constants for base-pair opening in the wt P1 duplex were determined from ammonia-catalyzed imino proton exchange measurements. The effects of [NH_3] on R_{1a} of the imino protons of the P1 helix were measured by inversion recovery experiments and results for the G23 and G25 imino protons are shown in Figure 3. From these data, the base-pair lifetimes ($\tau_0 = 1/k_{op}$) (C-2·G23: 31 ± 9 ms; C-4·G25: 9 ± 7 ms) and apparent equilibrium constants for opening (αK_{op}) (C-2·G23: $0.30 \pm 0.06 \times 10^{-6}$; C-4·G25: $0.36 \pm 0.06 \times 10^{-6}$) were determined by curve fitting using Equation (7). The R_{1a} data for the G25 imino proton show an almost linear correlation with [NH_3] in Figure 3, indicating that k_{cl} is significantly larger than αk_i[NH_3] [see Equation (7)]. These conditions lead to the large error in τ_0 for C-4·G25. Thus, a more conservative interpretation of the data for the C-4·G25 base pair is that $\tau_0 \leq 9$ ms. The data for C-2·G23 can be used to calculate an apparent lifetime for base-pair opening, $\alpha\tau_{open}$, of 9 ± 3 ns (using $\alpha\tau_{open} = \tau_0 \alpha K_{op}$). Except for G23 and G25, the other imino protons showed substantial line broadening for [NH_3] >30 mM (data not shown); thus, the lifetimes and equilibrium constants for opening of these base pairs could not be determined from the NH_3 data.

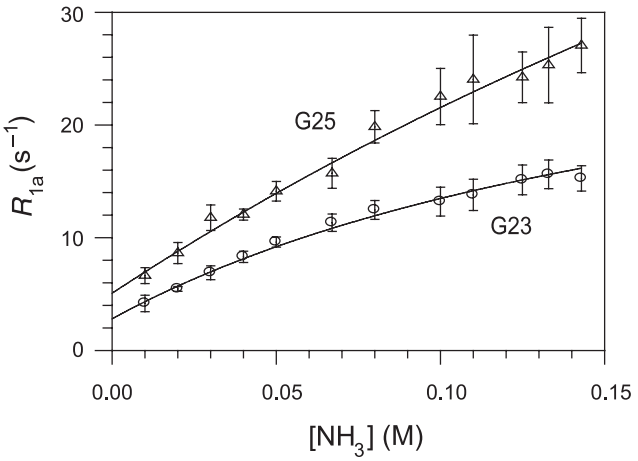

Figure 3. Ammonia-catalyzed exchange of the P1 duplex. Apparent spin-lattice R_1 relaxation rate constants (R_{1a}) of the G23 and G25 imino protons as a function of the ammonia concentration in NMR buffer at 35°C and pH 8.0. The NH_3 concentration was calculated by $[NH_3] = [NH_3]_{total}/(1 + 10^{(pKa-pH)})$, where $[NH_3]_{total}$ is the total concentration of ammonia added. The solid lines are the best fits to single exponential, and the error bars represent curve fitting errors during the determination of R_{1a} from inversion recovery data.

HPO_4^{2-} is a much weaker catalyst than ammonia and was also used to determine K_{op} for the base pairs. The R_{1a} values of the imino protons of the P1 duplex dissolved in the 10 mM sodium phosphate NMR buffer were measured at three different pHs, leading to different concentrations for the base catalyst HPO_4^{2-}. The phosphate tribasic anion precipitates with Mg^{2+} (K_{sp} of $Mg_3(PO_4)_2$ is $\sim 10^{-24}$) (37); thus, only three data points were collected here due to precipitation at higher concentrations of the phosphate buffer or higher pH with 10 mM phosphate buffer. As predicted from Equation (8), Figure 4A shows that R_{1a} increases linearly as a function of the HPO_4^{2-} concentration. However, the limited number of HPO_4^{2-} concentrations, combined with the fact that HPO_4^{2-} is a much weaker catalyst than ammonia, allowed only a qualitative interpretation of these data. As seen in Figure 4, base pairs C-5·G26 and U-3·A24 show the lowest dependence of R_{1a} on HPO_4^{2-} (and therefore smaller values for αK_{op}), C5·G18, A4·U19 and A3·U20 show intermediate αK_{op} values and both imino protons in the U-1·G22 base pair have the largest αK_{op} values. The R_{1a} for the U21 imino proton could not be determined because its resonance overlaps with the G18 resonance (see Figure 1B)

Base-pair stability and kinetics for the wt and modified P1 duplexes using TRIS as a base catalyst

TRIS base proved the most useful catalyst for these hydrogen exchange studies of the P1 duplexes because it was possible to measure the αK_{op} values for all non-terminal base pairs in the four P1 duplexes from analysis of the R_{1a} data using Equation (8) (Figure 5 and Table 1). These data were used to compare the effects of the modifications on base-pair stabilities. In the (-1C)-P1 duplex, where the central U-1·G22 base pair is changed to a C-1·G22 Watson–Crick base pair, exchange of the

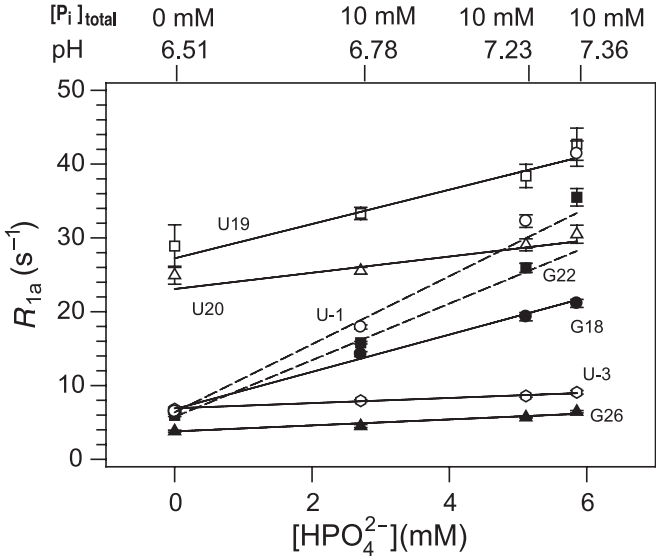

Figure 4. HPO_4^{2-}-catalyzed exchange experiments on the P1 duplex. The R_{1a} of the imino protons of the P1 duplex as a function of the HPO_4^{2-} concentration in NMR buffer at 35°C for G18 (filled circle), U19 (open square), U20 (open triangle), U-1 (open circle), G22 (filled square), U-3 (open hexagonal) and G26 (filled triangle). The concentration of HPO_4^{2-} was calculated from the pK_a for HPO_4^{2-} (7.21), the pH of the sample and the total phosphate concentration. The pH and $[P_i]_{total}$ for each condition are shown on top of the figure. The lines are fits of these data to Equation (8) where the R_{1a} data points were weighted by the inverse of their variance. The fits for U-1 and G22 imino protons are indicated by dashed lines and the other imino protons are indicated by solid lines. The error bars represent curve fitting errors during the determination of R_{1a} from inversion recovery data.

G22 imino proton shows much smaller dependence on TRIS concentration compared to the wt P1 duplex (Figure 5). This leads to a 200-fold smaller αK_{op} for the C-1·G22 base pair than the U-1·G22 base pair in the wt P1 duplex (Table 1), demonstrating that the G·U base pair is much less stable than a non-terminal Watson–Crick G·C base pairs. This difference in the base-pair stability between G·C and G·U base pairs also affects the stabilities of neighboring base pairs. The A2·U21 and A3·U20 base pairs in the (-1C)-P1 duplex have ~9- and 2.5-fold smaller αK_{op} values than those of the wt P1 duplex, respectively. However, there are no significant differences in the αK_{op} values between the two duplexes for the C-2·G23 and U-3·A24 base pairs on the other side of the G·U base pair. These results indicate that the change from G·U to G·C base pair in the RNA duplex leads to stabilization of this base pair as well as stabilization of base pairs on only one side of the modification.

Hydrogen exchange experiments were also performed for a duplex with a 2′-OMe modification at residue U-3 [termed here as (-3m)-P1]. The exchange of the U-3 imino protons showed a weaker dependence on TRIS compared to the wt P1 duplex, (Figure 5) leading to a 3-fold smaller calculated αK_{op} for the U-3·A24 base pair in the modified duplex (Table 1). There is no significant effect of this modification on the stabilities of the neighboring C-2·G23 and C-4·G25 base pairs (Figure 5 and Table 1). The 2′-OMe modification at the U-3 position caused only a small effect on the exchange of U-1 and G22 imino protons with TRIS buffer (Figure 5), where the αK_{op} of

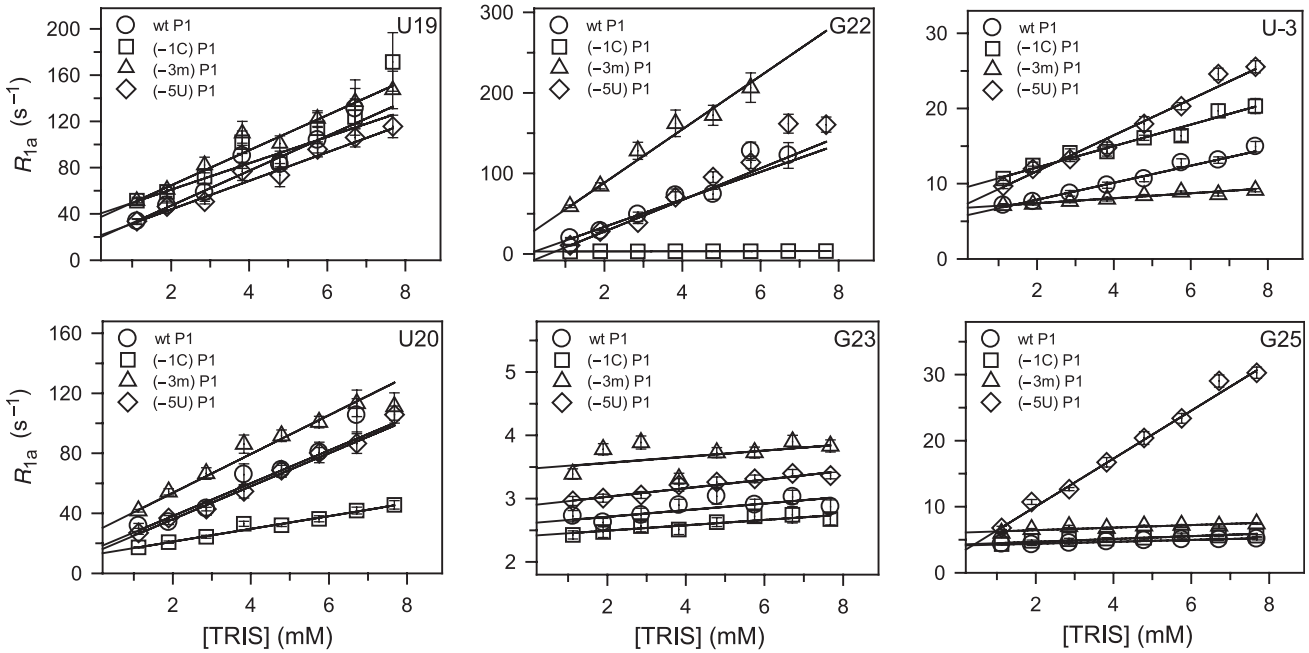

Figure 5. TRIS-catalyzed hydrogen exchange data on the wt and modified P1 duplexes. The R_{1a} of the imino protons of the wt P1 (circle), (-1C)-P1 (square), (-3m)-P1 (triangle) and (-5U)-P1 (diamond) duplexes are shown as a function of the concentration of TRIS base at 35°C at pH 7.67. The concentration of the TRIS base was calculated using a $pK_a = 7.87$ at 35°C and knowing the pH and total concentration of TRIS. The lines are the best fits of these data to Equation (8) where the R_{1a} data points were weighted by the inverse of their variance. The imino protons are labeled in the upper right corner of each figure. The error bars represent curve fitting errors during the determination of R_{1a} from inversion recovery data.

Table 1. Apparent base-pair dissociation constants (αK_{op}) of the wt and mutant P1 duplexes determined by the TRIS-catalyzed NMR exchange experiments at 35°C[a]

Base pair	Imino		P1 duplexes			
			wt	−1 C	−3 m	−5 U
Y-5·G26[b]	G26	αK_{op} ($\times 10^{-6}$)	31 ± 1	40 ± 1[c]	30 ± 2	n.d.[d]
C-4·G25	G25	αK_{op} ($\times 10^{-6}$)	<3.5 (0.36)	<3.5	<3.5	58 ± 2
U-3·A24	U-3	αK_{op} ($\times 10^{-6}$)	17 ± 1	21 ± 2	5.0 ± 0.4	35 ± 2
C-2·G23	G23	αK_{op} ($\times 10^{-6}$)	<1.5 (0.30)	<1.5	<1.5	<1.5
Y-1·G22[b]	U-1	αK_{op} ($\times 10^{-6}$)	300 ± 12	n.a.[e]	630 ± 32	280 ± 6
	G22	αK_{op} ($\times 10^{-6}$)	275 ± 16	1.2 ± 0.3	530 ± 34	315 ± 9
A2·U21	U21	αK_{op} ($\times 10^{-6}$)	740 ± 210[f]	83 ± 3	n.d.[f]	n.d.[f]
A3·U20	U20	αK_{op} ($\times 10^{-6}$)	160 ± 12	63 ± 3	190 ± 8	160 ± 7
A4·U19	U19	αK_{op} ($\times 10^{-6}$)	220 ± 20	170 ± 17	220 ± 15	180 ± 12
C5·G18	G18	αK_{op} ($\times 10^{-6}$)	270 ± 13[c]	380 ± 18	340 ± 11[c]	290 ± 7[c]

[a]Parameters used in the calculation: $k_{coll} = 1.5 \times 10^9\ s^{-1}$, pK_a(G-NH1) = 9.24, pK_a(U-NH3) = 9.20, pK_a(TRIS, 35°C) = 7.87; Sample conditions: 10 mM $MgCl_2$, 100 mM NaCl, 0.1 mM EDTA, $[TRIS]_{total}$ = 1–20 mM, 35°C. The pH of all samples and buffer were adjusted to 8.00 at 23.4°C and then calibrated to 7.67 at 35°C using the equation, pH(35°C) = pH(23.4°C)−0.033 × (35−23.4). The errors for these αK_{op} values were determined from the linear curve fitting using Equation (8). The αK_{op} values determined using ammonia as the catalyst are shown in parenthesis.
[b]Y indicates C or U.
[c]These resonances are partially overlapped with another resonance and this overlap may lead to a systematic error in αK_{op}. Thus these values may actually have larger errors than what are given, which only represent the errors derived from the fits.
[d]Not determined. The U-5·G26 base pair caused severe line broadening of G26 imino resonance.
[e]There is no resonance in the (-1C)-P1 duplex.
[f]The U21 imino resonances in the P1 duplexes, except the (-1C)-P1 duplex, showed line broadening and overlap with the G18 imino resonances. Thus, these values have larger errors or could not be determined.

the U-1·G22 base pair is ~2-fold larger for the (-3m)-P1 than the wt P1 duplex (Table 1).

The (-5U)-P1 duplex has a wobble pair at U-5·G26 and both the U-5 and G26 imino protons exchanged rapidly with water at 35°C so their resonances were not observed. This effect of the U-5·G26 base pair in the (-5U)-P1 duplex propagated to the C-4·G25 and U-3·A24 base pairs (Figure 5) but had little or no effect on the C-2·G23 and U-1·G22 base pairs (Figure 5 and Table 1).

DISCUSSION

NMR hydrogen exchange experiments have been used to probe the thermodynamics and kinetics for base-pair opening in a variety of nucleic acid systems (30). Most hydrogen exchange studies on nucleic acids are performed at or below room temperature in order to slow the observed exchange rates. However, the P1 duplex studied here showed evidence of aggregation at lower temperatures, so the hydrogen exchange kinetics was measured at 35°C. Ammonia is the most commonly used base catalyst in hydrogen exchange studies of nucleic acids (23,30); however, the high catalytic efficiency of the ammonia ($pK_a = 9.30$) led to rapid exchange for most of the imino protons at 35°C. Thus, the base-pair opening lifetimes and αK_{op} values could only be determined for the two most stable base pairs C-2·G23 and C-4·G25 using ammonia as the catalyst. Two other weaker base catalysts, TRIS base ($pK_a^{35°C} = 7.88$) and HPO_4^{2-} ($pK_a = 7.21$) were also employed here to determine αK_{op} values for other base pairs of the P1 duplex (33). For exchange data with both TRIS base and HPO_4^{2-}, the rate constant for base-pair closing, k_{cl}, is much larger than $\alpha k_i[B]$, so the measured R_{1a} is a simple linear function of the base catalyst [Equation (8) and Figures 4 and 5]. The imino protons of G23 and G25 showed only a small change in R_{1a} as a function of HPO_4^{2-} (data not shown) which is consistent with small αK_{op} values.

Hydrogen exchange experiments can also provide data on opening and closing rates of base pairs (30). The base-pair life times ($\tau_0 = 1/k_{op}$) at 35°C using ammonia as the catalyst could only be determined for the C-2·G23 and C-4·G25 base pairs in the P1 helix and were 31 and 9 ms, respectively. The open lifetimes for all other base pairs were too fast to measure (<1 ms) under the conditions employed here.

The exchange rates of the imino protons in nucleic acids are affected by both intrinsic and external base catalysts (30). In Figures 4 and 5, the slope of the linear correlation between R_{1a} of the imino proton and the concentration of the added catalyst is $\alpha k_i K_{op}$ and the y-intercept is $R_1 + K_{op} k_{tr,open}^{ACC}$ under experimental condition, where k_{cl} is much larger than $k_{tr,open}^{ACC}$ [see Equations (4) and (8)]. Thus, the imino proton of a less stable base pair with larger K_{op} will have both a larger slope and larger y-intercept in these plots. This pattern is followed for most of the imino protons, but not the two imino protons of the U-1·G22 wobble pair (see Figure 4 and Table 1). For example, although αK_{op} of the U-1·G22 wobble pair is larger than those of the A3·U20 and A4·U19 base pairs (Table 1), the imino protons of U-1 and G22 have the larger slopes but much smaller values of y-intercepts than these two A·U base pairs (Figure 4). This phenomenon is consistent with a different rate of internal catalysis ($k_{tr,open}^{ACC}$) for a U·G base pair compared to a standard Watson–Crick base pair. In a U·G wobble base pair, the hydrogen bond acceptors of U and G imino protons are carbonyl oxygens which are less basic and therefore

poorer base catalysts than the A-N1 or the C-N3 in standard base pairs (25,30,38).

The P1 duplex of *Tetrahymena* group I intron can be divided into three parts, the central U·G base pair, the AU-rich (region I; see Figure 1A), and the GC-rich (region II). The P1 duplex in the *Tetrahymena* L-21 ribozyme contains only the central U·G base pair and base pairs in region II, thus base pairing in region I is not required for activity (4). The αK_{op} data in Table 1 show that the central U-1·G22 base pair has a ~230-fold higher population of open states relative to having a C·G base pair at this position. Previous studies for opening of G·U and G·T base pairs in RNA and DNA duplexes showed that these wobble pairs have 10–100 times longer lifetimes in the open state than other Watson–Crick base pairs (25). These results are consistent with the thermodynamic data here and suggest that a large part of the destabilizing effect of the U-1·G22 is due to a longer lifetime for the open state.

The A2·U21 base pair is the least stable non-terminal Watson–Crick base pair in the P1 duplex. This base pair is not required for activity and even when this base pair forms, it has a very large αK_{op}. These results suggest that having a unstable base pair next to the central U-1·G22 pair (on the region I side) is important for the high catalytic activity. Previous studies have indicated that flexibility of the U-1·G22 base pair is important for the activity of the *Tetrahymena* ribozyme. For example, it was initially proposed that the U-1·G22 base pair interacts with the conserved A-rich J4/5-J5/4 symmetric loop, by a hydrogen bond between the NH_2 of G22 and the 2′-OH group of A207 at J5/4 (39). This tertiary interaction was subsequently observed in the crystal structures of the *Azoarcus* sp. and Twort group I introns, where the dT·G or U·G base pairs in the P1 duplex interacts with the 2′-OH of the A87 or A83, respectively (which are the same positions as A207 in the *Tetrahymena* ribozyme) (16,17). Formation of the tertiary interaction between G22 and A207 likely leads to destabilization of the U-1·G22 wobble. This is supported by the X-ray structure of Twort group I intron, which has a long hydrogen bonding distance (3.52 Å) between U-1-O2 and G8-N4 of the U-1·G8 wobble pair (equivalent to U-1·G22 wobble pair of *Tetrahymena* ribozyme). Changing the U-1·G22 wobble pair to a C-1·G22 base pair in the P1 duplex stabilizes this base pair to opening by over a factor of 200, and also stabilizes the A2·U21 base pair in region I by a factor of 9 (Table 1), but has little affect on stability of base pairs in region II. The results here show that the U-1·G22 and A·U base pairs in region I have high αK_{op} in the isolated P1 helix, suggesting that the dynamics of the isolated P1 duplex are tuned to help stabilize the active conformation in the docked state.

The results here also show that the destabilizing effect of the central U-1·G22 base pair is propagated asymmetrically to only one side of the duplex. The A2·U21 base pair on one side of the central U-1·G22 is the least stable (non-terminal) base pair but the C-2·G23 on the other side is the most stable base pair in the P1 duplex and is not affected by large αK_{op} for U-1·G22 (Table 1). Structural studies on RNA duplexes show asymmetric changes in the helical twist around U·G wobble base pairs (40–42). These RNA duplexes are unwound between the U·G wobble pair and the base pair 3′ to the U, but over-wound on the other side (40–42). Such helical unwinding on one side of the U·G wobble pair may lead to the large αK_{op} for A2·U21. The results here are also consistent with previous data on a DNA duplex where modification of a A·T base pair to a G·T wobble destabilized the G·C base pair on the 3′-side of the T more than the A·T base pair on the other side (25). However in this duplex there was still a relatively large effect on both sides of the wobble, with ~80-fold and 16-fold change in αK_{op} for base pairs on the 5′-side and 3′-side of the T, respectively. As seen in Table 1, there is a >30% change in αK_{op} for any of the base pairs on the 3′-side of U-1, but a ~9-fold change for the A2·U21 base pair on the 5′ side when comparing the wt to the (-1C)-P1 duplex. These difference could arise from comparing a DNA duplex to a RNA duplex, from difference sequences for the base pairs neighboring the G-U(T) wobble, or the different temperatures at which αK_{op} was measured. The (-5U)-P1 duplex studied here changes a G·C base pair in region II to a G·U base pair and the hydrogen exchange results showed enhanced opening for the G·U as well as the neighboring and next nearest neighboring base pairs on the 3′ side of the U (Table 1). The stability of the base pair on the other side of the G·U pair could not be studied because the imino proton of this terminal base-pair exchanged with water too rapidly to be observed. The U-1·G22 wobble pair appears to be important for ribozyme activity where the enhanced opening and lower stability of this base pair aids the formation of tertiary interaction with A207, and the asymmetry around the U-1·G22 base pair can help stabilize base pairs in region II. The data are also consistent with a model that a reduced undocking rate of the P1 duplex, arising from formation of the tertiary interaction between G22 and A207 (7,39), is thermodynamically linked to the instability of the U-1·G22 base pair at the cleavage site.

The hydrogen exchange studies here showed that 2′-OMe modification at U-3 leads to stabilization of the U-3·A24 base pair with ~4-fold smaller αK_{op}. This modification also causes a small 2-fold destabilization of the U-1·G22 two base pairs away, but had no measurable effect on the directly neighboring C-2·G23 and C-4·G25 base pairs. Previous studies of unmodified and fully modified, $r(CGCGCG)_2$, showed that 2′-O-methylation stabilized the duplex to thermal denaturation but had little effect on the NMR solution structure (43). The X-ray crystal and NMR solution structural studies of this duplex showed that the 2′-OMe group points towards the minor group (43–45) and is very close to the H5′ of the 3′-neighboring residue (43). The X-ray structure of the fully modified, $r(CGCGCG)_2$ duplex shows that the 2′-OMe group affects the minor groove hydration pattern (44,45), thus stabilization of the U-3·A24 base pair may arise from protection of the 2′-OMe group from water. Previous studies showed that a 2′-OMe modification at U-3 increased the undocking rate of the P1 duplex by ~140-fold (7). A 2′-deoxy modification at the same position also led to a ~30-fold increase in the undocking rate (7), even though the 2′-deoxy substitution at this position leads to lower thermal stability for the P1 duplex

($\Delta\Delta G^{\circ}$ $\approx$0.87 kcal/mol) (12). Both helical stabilization by a 2′-OMe modification and helical destabilization by a 2′-deoxy modification at U-3 increased the k_{undock} of the P1 duplex, indicating there is no correlation between the thermal stability of U-3·A24 base pair and docking of the P1 duplex. In the crystal structures of the Twort group I ribozyme-product complex (PDB ID: 1Y0Q) and *Azoarcus* sp. group I intron in complex with both exons (PDB ID: 1U6B), the 2′-OH group of residue C-3 in P1 helix (equivalent to U-3 of *Tetrahymena* ribozyme) is within hydrogen bonding distance of the N1 of G182 (2.97 Å) or A168 (2.67 Å), respectively. Although this position has no sequence homology in the group I intron (U300 in the *Tetrahymena* ribozyme, G182 in the Twort group I ribozyme and A168 in the *Azoarcus* sp. group I intron), the long-range hydrogen bond of the –3 position may still be important for determining the undocking rates. This hypothesis may explain why a 2′-H or 2′-OMe modification at U-3 strongly interferes with the tertiary interaction between the P1 duplex and catalytic core (7).

CONCLUSION

The thermodynamics and kinetics for base-pair opening in the P1 duplex of the *Tetrahymena* group I ribozyme were studied by NMR imino proton exchange experiments. C-2·G23 and C-4·G25 were the most stable base pairs in the P1 helix where the kinetics and thermodynamics for opening were determined at 35°C from analysis of exchange experiments using ammonia as a catalyst. The equilibrium constants for base-pair opening for the other more rapidly exchanging imino protons were determined using the weaker base catalyst, TRIS. These studies also revealed a high degree of asymmetry in the thermodynamics for opening of base pairs around the central U-1·G22 wobble pair, where base pairs on the 3′-side of the U were substantially destabilized whereas there was little effect on base pairs on the other side of the wobble. This asymmetry may result from the known asymmetry of the helical twist around G·U wobble pairs (40–42), which may lead to the a general phenomenon that replacement of a C·G with a U·G also leads to asymmetric destabilization of base pairs towards the 3′-side of U. The hydrogen exchange NMR studies here revealed an unusual pattern of base-pair stability for residues A2·U21, U-1·G22 and C-2·G23 in the P1 duplex and these results are consistent with the model that flexibility in the P1 duplex is important for forming stabilizing tertiary interactions with the catalytic core of the *Tetrahymena* ribozyme.

SUPPLEMENTARY DATA

Supplementary Data are available at NAR Online.

ACKNOWLEDGEMENTS

This work was supported by grants from NIH (AI 30726) to A.P. and the Korea Research Foundation Grant funded by the Korea Government (MOEHRD, Basic Research Promotion Fund) (KRF-2006-331-C00188) to J.-H.L. Funding to pay the Open Access publication charges for this article was provided by the same sources.

Conflict of interest statement. None declared.

REFERENCES

1. Cech,T.R. (1993) Structure and mechanism of the large catalytic RNAs: Group I and Group II introns and ribonuclease P. In: Gesteland,R.F. and Atkins,J.F. (eds), *The RNA World*. Cold Spring Harbor Laboratory Press, NY, pp. 239–269.
2. Shan,S.-O. and Herschlag,D. (2002) Dissection of a metal-ion-mediated conformational change in *Tetrahymena* ribozyme catalysis. *RNA*, **8**, 861–872.
3. Karbstein,K., Carroll,K.S. and Herschlag,D. (2002) Probing the *Tetrahymena* group I ribozyme reaction in both directions. *Biochemistry*, **41**, 11171–11183.
4. Been,M.D. and Cech,T.R. (1986) One binding-site determines sequence specificity of *Tetrahymena* pre-ribosomal-RNA self-splicing, transsplicing, and RNA enzyme-activity. *Cell*, **47**, 207–216.
5. Pyle,A.M. and Cech,T.R. (1991) Ribozyme recognition of RNA by tertiary interactions with specific ribose 2′-OH groups. *Nature*, **350**, 628–631.
6. Pyle,A.M., McSwiggen,J.A. and Cech,T.R. (1990) Direct measurement of oligonucleotide substrate binding to wild-type and mutant ribozymes from *Tetrahymena*. *Proc. Natl Acad. Sci. USA*, **87**, 8187–8191.
7. Bartley,L.E., Zhuang,X., Das,R., Chu,S. and Herschlag,D. (2003) Exploration of the transition state for tertiary structure formation between an RNA helix and a large structured RNA. *J. Mol. Biol.*, **328**, 1011–1026.
8. Shan,S.-O., Kravchuk,A.V., Piccirilli,J.A. and Herschlag,D. (2001) Defining the catalytic metal ion interactions in the *Tetrahymena* ribozyme reaction. *Biochemistry*, **40**, 5161–5171.
9. Shan,S.-O. and Herschlag,D. (2000) An unconventional origin of metal-ion rescue and inhibition in the *Tetrahymena* group I ribozyme reaction. *RNA*, **6**, 795–813.
10. Shan,S.-O., Yoshida,A., Sun,S., Piccirilli,J.A. and Herschlag,D. (1999) Three metal ions at the active site of the *Tetrahymena* group I ribozyme. *Proc. Natl Acad. Sci. USA*, **96**, 12299–12304.
11. Yoshida,A., Sun,S. and Piccirilli,J.A. (1999) A new metal ion interaction in the *Tetrahymena* ribozyme reaction revealed by double sulfur substitution. *Nat. Struct. Biol.*, **6**, 318–321.
12. Narlikar,G.J., Khosla,M., Usman,N. and Herschlag,D. (1997) Quantitating tertiary binding energies of 2′ OH groups on the P1 duplex of the *Tetrahymena* ribozyme: intrinsic binding energy in an RNA enzyme. *Biochemistry*, **36**, 2465–2477.
13. Bevilacqua,P.C., Sugimoto,N. and Turner,D.H. (1996) A mechanistic framework for the second step of splicing catalyzed by the *Tetrahymena* ribozyme. *Biochemistry*, **35**, 648–658.
14. Sugimoto,N., Tomka,M., Kierzek,R., Bevilacqua,P.C. and Turner,D.H. (1989) Effects of substrate structure on the kinetics of circle opening reactions of the self-splicing intervening sequence from *Tetrahymena thermophila*: evidence for substrate and Mg^{2+} binding interactions. *Nucleic Acids Res.*, **17**, 355–371.
15. Herschlag,D. and Cech,T.R. (1990) Catalysis of RNA cleavage by the *Tetrahymena thermophila* ribozyme. 1. Kinetic description of the reaction of an RNA substrate complementary to the active site. *Biochemistry*, **29**, 10159–10171.
16. Adams,P.L., Stahley,M.R., Kosek,A.B., Wang,J. and Strobel,S.A. (2004) Crystal structure of a self-splicing group I intron with both exons. *Nature*, **430**, 45–50.
17. Golden,B.L., Kim,H. and Chase,E. (2005) Crystal structure of a phage Twort group I ribozyme-product complex. *Nat. Struct. Mol. Biol.*, **12**, 82–89.
18. Guo,F., Gooding,A.R. and Cech,T.R. (2004) Structure of the *Tetrahymena* ribozyme: base triple sandwich and metal ion at the active site. *Mol. Cell*, **16**, 351–362.

19. Vicens,Q. and Cech,T.R. (2006) Atomic level architecture of Group I introns revealed. *Trends Biochem. Sci.*, **31**, 41–51.
20. Stahley,M.R. and Strobel,S.A. (2006) RNA splicing: group I intron crystal structures reveal the basis of splice site selection and metal ion catalysis. *Curr. Opin. Struct. Biol.*, **16**, 319–326.
21. Snoussi,K. and Leroy,J.-L. (2002) Alteration of A.T base-pair opening kinetics by the ammonium cation in DNA A-tracts. *Biochemistry*, **41**, 12467–12474.
22. Folta-Stogniew,E. and Russu,I.M. (1996) Base-catalysis of imino proton exchange in DNA: effects of catalysts upon DNA structure and dynamics. *Biochemistry*, **35**, 8439–8449.
23. Wärmländer,S., Sen,A. and Leijon,M. (2000) Imino proton exchange in DNA catalyzed by ammonia and trimethylamine: evidence for secondary long-lived open state of the base pair. *Biochemistry*, **39**, 607–615.
24. Wärmländer,S., Sandström,K., Leijon,M. and Gräslund,A. (2003) Base-pair dynamics in an antiparallel DNA triplex measured by catalyzed imino proton exchange monitored via ^{1}H NMR spectroscopy. *Biochemistry*, **42**, 12589–12595.
25. Varnai,P., Canalia,M. and Leroy,J.-L. (2004) Opening mechanism of G.T/U pairs in DNA and RNA duplexes: a combined study of imino proton exchange and molecular dynamics simulation. *J. Am. Chem. Soc.*, **126**, 14659–14667.
26. Nonin,S., Jiang,F. and Patel,D.J. (1997) Imino proton exchange and base pair kinetics in the AMP-RNA aptamer complex. *J. Mol. Biol.*, **268**, 359–374.
27. Dhavan,G.M., Lapham,J., Yang,S. and Crothers,D.M. (1999) Decreased imino proton exchange and base-pair opening in the IHF-DNA complex measured by NMR. *J. Mol. Biol.*, **288**, 659–671.
28. Cao,C., Jiang,Y.L., Stivers,J. and Song,F. (2004) Dynamic opening of DNA during the enzymatic search for a damaged base. *Nat. Struct. Mol. Biol.*, **11**, 1230–1236.
29. Snoussi,K. and Leroy,J.-L. (2001) Imino proton exchange and base-pair kinetics in RNA duplexes. *Biochemistry*, **40**, 8898–8904.
30. Guéron,M. and Leroy,J.-L. (1995) Studies of base pair kinetics by NMR measurement of proton exchange. *Methods Enzym.*, **261**, 383–413.
31. Leroy,J.-L., Bolo,N., Figueroa,N., Plateau,P. and Guéron,M. (1985) Internal motions of transfer RNA: a study of exchanging protons by magnetic resonance. *J. Biomol. Struct. Dyn.*, **2**, 915–939.
32. Milligan,J.F., Broebe,D.R., Witherell,G.W. and Uhlenbeck,O.C. (1987) Oligoribonucleotide synthesis using T7 RNA polymerase and synthetic DNA templates. *Nucleic Acids Res.*, **15**, 8783–8798.
33. Mohan,C. (2003) *Buffers: A Guide for the Preparation and Use of Buffers in Biological Systems*. CalBiochem, Darmstadt, Germany.
34. Delaglio,F., Grzesiek,S., Vuister,G.W., Zhu,G., Pfeifer,J. and Bax,A. (1995) NMRPipe: a multidimensional spectral processing system based on UNIX pipes. *J. Biomol. NMR*, **6**, 277–293.
35. Goddard,T.D. and Kneller,D.G. (2003) SPARKY 3. University of California, San Francisco, CA.
36. Liu,M., Mao,X., Ye,C., Huang,H., Nicholson,J.K. and Lindon,J.C. (1998) Improved WATERGATE pulse sequences for solvent suppression in NMR spectroscopy. *J. Magn. Reson.*, **132**, 125–129.
37. Taylor,A.W., Frazier,A.W. and Gurney,E.L. (1963) Solubility products of magnesium ammonium and magnesium potassium phosphate. *Trans. Faraday Soc.*, **59**, 1580–1584.
38. Saenger,W. (1983) *Principles of Nucleic Acid Structure*. Springer, New York, NY.
39. Strobel,S.A., Ortoleva-Donnelly,L., Ryder,S.P., Cate,J.H. and Moncoeur,E. (1998) Complementary sets of noncanonical base pairs mediate RNA helix packing in the group I intron active site. *Nat. Struct. Biol.*, **5**, 60–66.
40. Trikha,J., Filman,D.J. and Hogle,J.M. (1999) Crystal structure of a 14 bp RNA duplex with non-symmetrical tandem G.U wobble base pairs. *Nucleic Acids Res.*, **27**, 1728–1739.
41. Mueller,U., Shchubel,H., Sprinzl,M. and Heinemann,U. (1999) Crystal structure of acceptor stem of tRNA(Ala) from Escherichia coli shows unique G.U wobble base pair at 1.16 Å resolution. *RNA*, **5**, 670–677.
42. Klinck,R., Westhof,E., Walker,S., Afshar,M., Collier,A. and Aboul-Ela,F. (2000) A potential RNA drug target in the hepatitis C virus internal ribozomal entry site. *RNA*, **6**, 1423–1431.
43. Popenda,M., Biala,E., Milecki,J. and Adamiak,R.W. (1997) Solution structure of RNA duplexes containing alternating CG base pairs: NMR study of r(CGCGCG)$_2$ and 2′O-Me(CGCGCG)$_2$ under low salt condition. *Nucleic Acids Res.*, **25**, 4589–4598.
44. Adamiak,D.A., Rypniewski,W.R., Milecki,J. and Adamiak,R.W. (2001) The 1.19 Å X-ray structure of 2′-O-Me(CGCGCG)$_2$ duplex shows dehydrated RNA with 2-methyl-2,4-pentanediol in the minor groove. *Nucleic Acids Res.*, **29**, 4144–4153.
45. Adamiak,D.A., Milecki,J., Popenda,M., Adamiak,R.W., Dauter,Z. and Rypniewski,W.R. (1997) Crystal structure of 2′-O-Me(CGCGCG)$_2$, an RNA duplex at 1.30 Å resolution. Hydration pattern of 2′-O-methylated RNA. *Nucleic Acids Res.*, **25**, 4599–4607.